Downloaded from rsta.royalsocietypublishing.org on 13 July 2009

PHILOSOPHICAL TRANSACTIONS OF THE ROYAL SOCIETY A MATHEMATICAL, PHYSICAL & ENGINEERING SCIENCES

Cyclotron resonance of electrons and holes in graphene monolayers

Kai-Chieh Chuang, Russell S Deacon, Robin J Nicholas, Kostya S Novoselov and Andre K Geim

Phil. Trans. R. Soc. A 2008 **366**, 237-243
doi: 10.1098/rsta.2007.2158

References **This article cites 20 articles, 1 of which can be accessed free**
http://rsta.royalsocietypublishing.org/content/366/1863/237.full.html#ref-list-1

Rapid response Respond to this article
http://rsta.royalsocietypublishing.org/letters/submit/roypta;366/1863/237

Email alerting service Receive free email alerts when new articles cite this article - sign up in the box at the top right-hand corner of the article or click **here**

To subscribe to *Phil. Trans. R. Soc. A* go to:
http://rsta.royalsocietypublishing.org/subscriptions

This journal is © 2008 The Royal Society

Downloaded from rsta.royalsocietypublishing.org on 13 July 2009

PHILOSOPHICAL TRANSACTIONS OF THE ROYAL SOCIETY A

Phil. Trans. R. Soc. A (2008) **366**, 237–243
doi:10.1098/rsta.2007.2158
Published online 19 November 2007

Cyclotron resonance of electrons and holes in graphene monolayers

By Kai-Chieh Chuang[1], Russell S. Deacon[1], Robin J. Nicholas[1,*], Kostya S. Novoselov[2] and Andre K. Geim[2]

[1]*Department of Physics, Clarendon Laboratory, Oxford University, Parks Road, Oxford OX1 3PU, UK*
[2]*Manchester Centre for Mesoscience and Nanotechnology, University of Manchester, Manchester M19 9PL, UK*

We report studies of cyclotron resonance in monolayer graphene. Cyclotron resonances are detected by observing changes in the photoconductive response of the sample. An electron velocity at the Dirac point of 1.093×10^6 m s^{-1} is obtained, which is the fastest velocity recorded for all known carbon materials. In addition, a significant asymmetry exists between band structure for electrons and holes, which gives rise to a 5% difference between the velocities at energies of 125 meV away from the Dirac point.

Keywords: graphene; cyclotron resonance; Fermi velocity

1. Introduction

Ever since the isolation of graphene in 2004 (Novoselov *et al.* 2004), a vast amount of interest has been shown in this truly two-dimensional system in which a flat monolayer of carbon atoms are arranged in a honeycomb lattice. Owing to the two-dimensional nature of the material, graphene has a fascinating electronic band structure in which charge carriers behave as Dirac fermions with extremely high velocities due to the near-linear dispersion relations close to the *K*-point in the Brillouin zone. This results in the observation of new scientific phenomena such as chiral quantum Hall effects (Novoselov *et al.* 2005; Zhang *et al.* 2005, 2006) as well as realistic potential for applications in high-speed electronics (Geim & Novoselov 2007). Theoretically, the study of graphene began in 1947 (Wallace 1947), but it is only very recently that measurements of the electron velocities were performed on monolayers of graphene (Deacon *et al.* 2007; Jiang *et al.* 2007). Close to the *K*-point, the graphene dispersion relation takes the form $E-E_{\mathrm{F}}=\pm c^*\hbar k$, where c^* is the velocity of charge carriers, and crosses over at the Fermi energy, indicating that graphene is a zero-gap semiconductor with symmetric bands. Applying a magnetic field to graphene leads to the formation of Landau levels (McClure 1956; figure 1) given by

$$E_n=\mathrm{sgn}(N)\times c^*\sqrt{2e\hbar B|N|}, \tag{1.1}$$

* Author for correspondence (r.nicholas@physics.ox.ac.uk).

One contribution of 11 to a Discussion Meeting Issue ‘Carbon-based electronics: fundamentals and device applications’.

 This journal is © 2007 The Royal Society

Downloaded from rsta.royalsocietypublishing.org on 13 July 2009

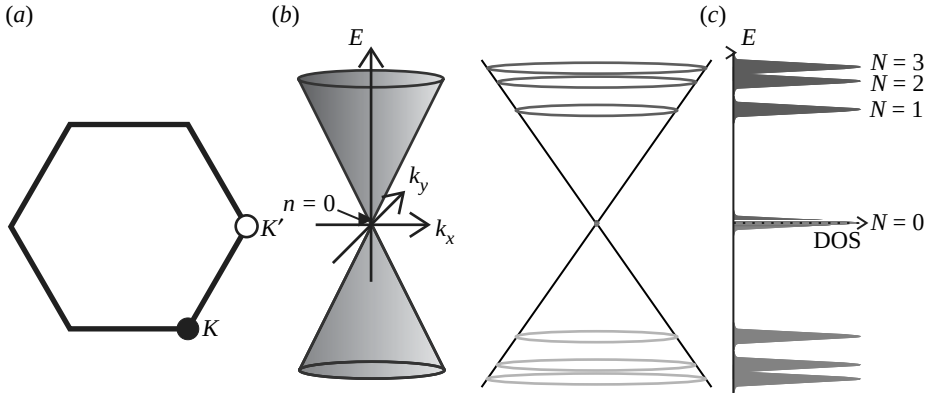

Figure 1. (*a*) Brillouin zone of graphene with two inequivalent lattice points, K and K'. (*b*) Linear dispersion relation of graphene, forming Dirac cones above and below the Dirac point. (*c*) Formation of Landau levels for monolayer of graphene upon the application of a magnetic field showing the density of states (DOS).

where $|N|$ is the Landau quantum index and B is the magnetic field. This allows us to make precise measurements of the electron (hole) velocity near the Fermi energy by studying the cyclotron resonance of graphene monolayers, in which a significant asymmetry between the electron and hole bands is observed, in contrast to the prediction of simple tight-binding theory (Saito *et al.* 1992; Reich *et al.* 2002).

2. Experimental details

Graphene monolayer samples were produced by micromechanical cleavage of bulk graphite onto a SiO_2/Si wafer with multiple electrodes contacted onto the graphene monolayer by conventional microfabrication. The samples were characterized by studying Shubnikov–de Haas oscillations to confirm that they were single layers, as multilayer graphenes have a more complex dispersion relation (McCann & Fal'ko 2006; Novoselov *et al.* 2006); this process also allowed us to verify the relationship between gate voltage and carrier densities. Experiments were carried out by studying the changes of the photoconductivity for graphene samples when illuminated with infrared radiation produced by a CO_2 laser, with energies between 115 and 135 meV. The typical laser power densities were approximately $3\times10^4\,\mathrm{Wm}^{-2}$, meaning the power on the samples is roughly 5 μW. The experiments were set up in the Faraday geometry, where incident radiation is normal to the samples and parallel to magnetic field, as shown in figure 2*b*. Samples were immersed in liquid helium at 1.5 K, a current of $I=100$ nA was supplied to the samples with data collected in a two-contact configuration as this gives qualitatively similar response compared with a four-contact configuration, but much better signal-to-noise ratio. The magnitude of the photoresponse signal is related to the amount of light absorbed by the sample, and hence is directly related to the absorption coefficient, with the greatest positive signals detected at Landau-level occupancy $\nu=nh/eB$ at -3.0, -0.76, 0.88 and 3.1; 0 being the Dirac point. This demonstrates that the

Downloaded from rsta.royalsocietypublishing.org on 13 July 2009

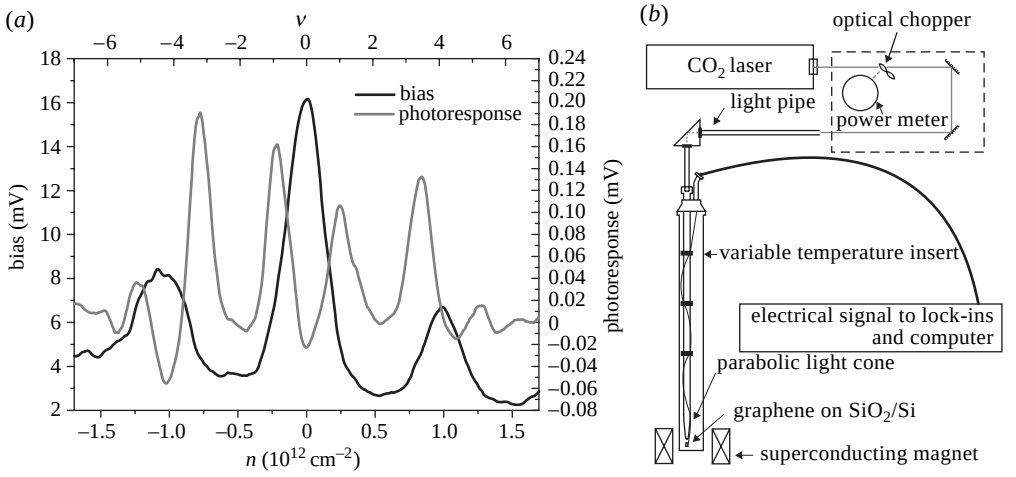

Figure 2. (*a*) Density dependence of the two-contact resistive voltage and photoconductive response of a typical graphene sample for infrared radiation of 117 meV at 10 T. (*b*) Schematic of the experimental set-up.

photoconductive signals show a derivative behaviour, with large positive signals observed at the edges of the conductance peaks, at the points where resistivity changes most rapidly with temperature and chemical potential. The peaks are assigned as $1-$, $0-$, $0+$ and $1+$ transitions, respectively, and the transitions take place from the Dirac point ($N=0$) to the $N=-1(+1)$ Landau level, as holes (electrons) absorb a photon. The $1-$ and $1+$ peaks are pure hole and electron transitions, whereas both $0-$ and $0+$ peaks contain contributions from both transitions but with one type of charge carriers more dominant than the other.

By sweeping charge carrier density at each value of magnetic field and recording the photoconductivity at each point, we were able to identify resonant cyclotron transitions for pure and mixtures of hole- and electron-like transitions. In order to produce full resonances to accurately measure the resonance positions, traces of photoconductive signals were then taken at fixed Landau-level occupancies following the lines shown in figure 3*b*. A typical trace taken at laser energy of 135 meV is shown in figure 3*c*, with Lorentzian fitting shown as the red line.

3. Results and discussion

Evidence of cyclotron resonance can be observed easily with this set-up, large photoconductive voltage variations as high as 3% can be seen at resonance, with the data suggesting a significant difference in resonance positions for the electrons and holes. The fixed occupancy traces showing the resonances are then fitted with conventional Lorentzian lineshapes with a linear background to correct for the bolometric response caused by strong localization of the carriers at high field.

Figure 4 shows the resonance positions plotted as a function of magnetic field and immediately a clear splitting between electron- and hole-like resonances can be seen, which equation (1.1) does not predict. Fitting velocities to each of the

Downloaded from rsta.royalsocietypublishing.org on 13 July 2009

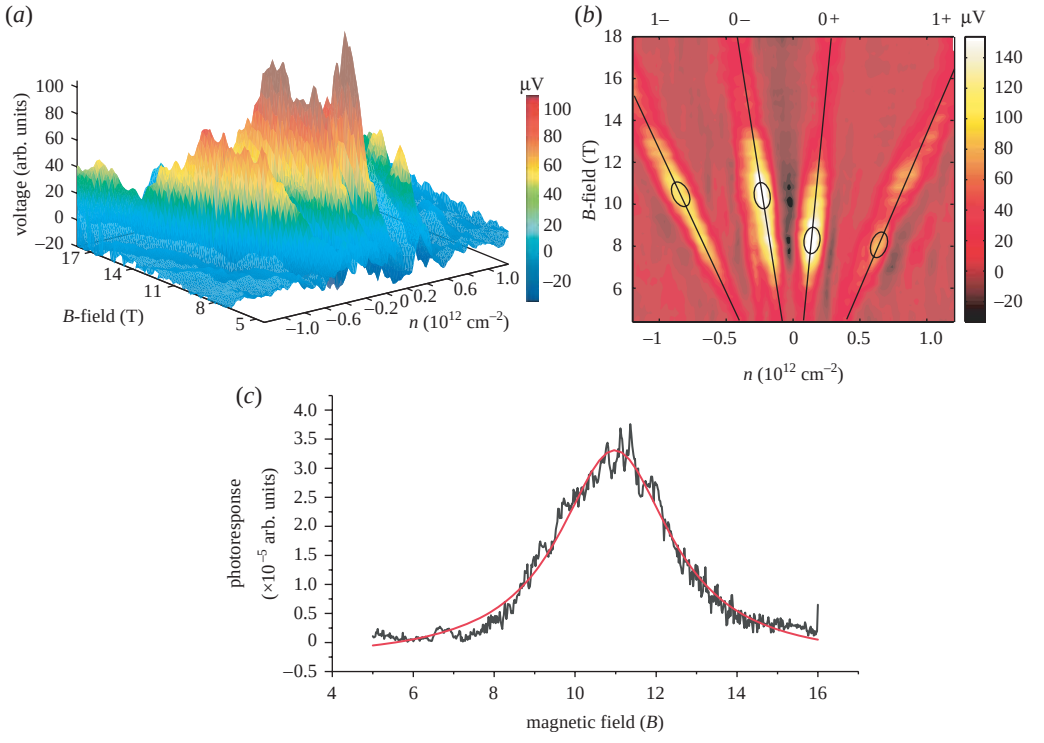

Figure 3. (*a*) Three-dimensional photoconductive response map as a function of carrier density and magnetic field for 121 meV. (*b*) Contour plot of the same set of data; the lines and ellipses are rough guides for the eyes only. (*c*) Typical trace signal for the 0+ resonance taken as a function of magnetic field, at laser energy 135 meV with the carrier densities scanned to keep the occupancies constant. The red line shows the Lorentzian fit.

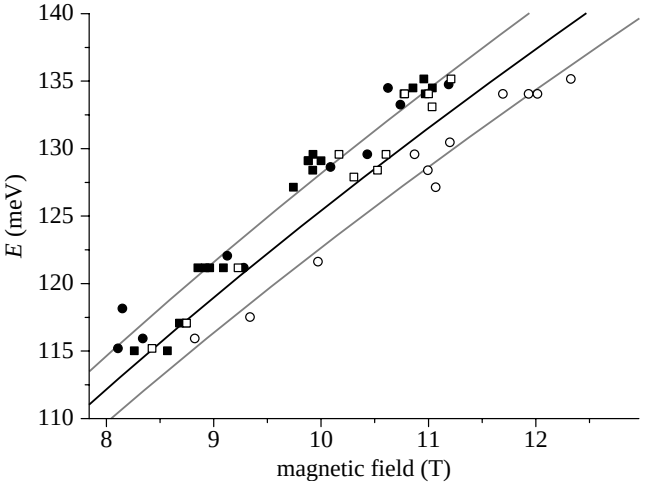

Figure 4. Resonance positions for the four resonances as a function of B. The grey lines are fitted velocities for the pure electron and hole transitions. The black line is the velocity fitted when combining the two pure transitions (filled square, $n+0$; filled circle, $n+1$; open square, $n-0$; open circle, $n-0$).

Downloaded from rsta.royalsocietypublishing.org on 13 July 2009

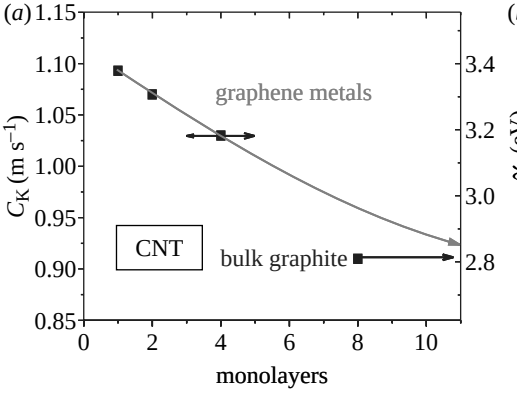

(b)

system	C_K ($\times 10^6$ m s^{-1})	γ_0 (eV)
theory[a]	0.87–1	2.7–3.1
carbon nanotubes[b]	0.9–0.94	2.8–2.9
graphite: ARPES[c]	0.91	2.81
epitaxial graphite (3–5) layers[d]	1.03	3.18
bilayer graphene[e]	1.07	3.31
monolayer graphene	1.093	3.38

Figure 5. (*a*) Fermi velocity at Dirac point plotted as a function of number of graphene layers; (*b*) data points are summarized in the table with the corresponding γ_0 for each system. CNT, carbon nanotube. [a]Saito *et al.* (1992, 1998), Reich *et al.* (2002); [b]Filho *et al.* (2004); [c]Zhou *et al.* (2006); [d]Sadowski *et al.* (2006); [e]Li & Andrei (2007).

resonances separately gives values of $c^* = (1.117, 1.118, 1.105, 1.069 \pm 0.004) \times 10^6$ m s^{-1} for the $1+$, $0+$, $0-$, $1-$ resonances, respectively. Nearest-neighbour tight-binding theory (Saito *et al.* 1998) predicts the dispersion relation of graphene in terms of the carbon–carbon interaction energy γ_0 and the overlap integral s_0, and close to the Dirac point, this gives the electron velocity as

$$c_{\pm}^* = c_K^* \frac{1}{1 \mp \frac{s_0 E}{\gamma_0}}, \tag{3.1}$$

where $c_K^* = (\sqrt{3}/2)(\gamma_0 a_0/\hbar)$. First-principle calculations (Saito *et al.* 1998) typically give $\gamma_0 = 3.03$ eV, $s_0 = 0.129$ and $c_K^* = 0.98 \times 10^6$ m s^{-1} with other reports in the regime $\gamma_0 = 2.7 - 3.1$ eV (Reich *et al.* 2002). Fitting the data in figure 4 to this relation gives $c_K^* = 1.093 \times 10^6$ m s^{-1} at the Dirac point, corresponding to $\gamma_0 = 3.38$ eV, with $s_0 = 0.6 \pm 0.1$. The unusually large fitted value for $s_0 = 0.6 \pm 0.1$ reflects the large asymmetry observed for electron and hole velocities. The value for c_K^* agrees with Jiang's direct cyclotron resonance results (2007) and is significantly greater than the values reported for previous studies of the Fermi velocities for graphite and multilayers of graphene sheets in metallic systems (Sadowski *et al.* 2006; Zhou *et al.* 2006; Li & Andrei 2007). Plotting the Fermi velocities as a function of the number of graphene layers, it can be seen that the Fermi velocity falls by approximately 20% between monolayer graphene and bulk graphite, as shown in figure 5, whereas the value of approximately 2.9 eV deduced from the band structure of semiconducting carbon nanotubes (Filho *et al.* 2004) still corresponds with values deduced from the theoretical and graphite values of γ_0. This progressive increase of electron velocity as numbers of graphene layers decrease suggests that the π bonds which are normal to the graphene surface have an important role in determining the Fermi velocity, as these bonds are directly responsible for the interlayer coupling and the coupling to the SiO_2 layer. A similar situation was observed in a recent report on filling carbon nanotubes with crystalline material (Li *et al.* 2006) in which it was suggested that the coupling between the carbon atoms and manganese telluride increases the transfer integral.

Downloaded from rsta.royalsocietypublishing.org on 13 July 2009

The origin of the large asymmetry between electrons and holes is still not well understood, as the tight-binding model predicts a difference of only 1% in total between the hole and electron velocities at $E \approx 125$ meV with the actual observed difference being five times larger. However, all the analysis used is based on single-particle theory and it is possible that many-body interactions could affect the quantities measured in this report. Although electron–electron interactions can be neglected for long-wavelength excitations for parabolic systems as stated by Kohn's theorem (Kohn 1961), linear systems such as single-layer graphene are predicted to show velocity renormalization effects from both electron–electron interactions (González *et al.* 1994) and electron–phonon coupling (Park *et al.* 2007).

4. Conclusion

We have successfully measured the Fermi velocity in monolayer graphene using cyclotron resonance, which is found to be considerably larger than that seen in thicker graphitic systems. We have shown that using photoconductivity gives significantly narrower linewidths than that observed in infrared absorption on large area samples (Jiang *et al.* 2007) which allows us to detect an asymmetry between the carrier velocity for the hole- and electron-like parts of the dispersion relation close to the Dirac point. The single-particle picture gives an adequate description of the broad outline of behaviour seen but does not provide an explanation for the asymmetry or the dependence on the number of graphene layers. These phenomena, together with observations such as the deviation of precise scaling for higher-order Landau level transitions (Jiang *et al.* 2007), suggest that many-body interactions may prove to be important in a full understanding of the behaviour of this system. Also the roles of spin splitting, valley splitting and excitonic interactions in this system still remain unanswered and may turn out to be very significant in providing a full description of the properties of monolayer graphene, as is the case for carbon nanotubes.

Part of this work has been supported by EuroMagNET under the EU contract RII3-CT-2004-506239 of the 6th Framework 'Structuring the European Research Area, Research Infrastructures Action'.

References

Deacon, R. S., Chuang, K.-C., Nicholas, R. J., Novoselov, K. S. & Geim, A. K. 2007 Cyclotron resonance study of the electron and hole velocity in graphene monolayers. *Phys. Rev. B* **76**, 081406. (doi:10.1103/PhysRevB.76.081406)

Filho, A. G. S. *et al.* 2004 Stokes and anti-Stokes Raman spectra of small-diameter isolated carbon nanotubes. *Phys. Rev. B* **69**, 115428. (doi:10.1103/PhysRevB.69.115428)

Geim, A. K. & Novoselov, K. S. 2007 The rise of graphene. *Nat. Mater.* **6**, 183–191. (doi:10.1038/nmat1849)

González, J., Guinea, F. & Vozmediano, M. A. H. 1994 Non-Fermi liquid behavior of electrons in the half-filled honeycomb lattice (a renormalization group approach). *Nucl. Phys. B* **424**, 595–618. (doi:10.1016/0550-3213(94)90410-3)

Jiang, A., Henriksen, E. A., Tung, L. C., Wang, Y.-J., Schwartz, M. E., Han, M. Y., Kim, P. & Stormer, H. L. 2007 Infrared spectroscopy of Landau levels of graphene. *Phys. Rev. Lett.* **98**, 197403. (doi:10.1103/PhysRevLett.98.197403)

Downloaded from rsta.royalsocietypublishing.org on 13 July 2009

Kohn, W. 1961 Cyclotron resonance and de Haas–van Alphen oscillations of an interacting electron gas. *Phys. Rev.* **123**, 1242–1244. (doi:10.1103/PhysRev.123.1242)

Li, G. & Andrei, E. Y. 2007 Observation of Landau levels of Dirac ferioms in graphite. (http://arxiv.org/abs/0705.1185)

Li, L.-J., Lin, T.-W., Doig, J., Mortimer, I. B., Wiltshire, J. G., Taylor, R. A., Sloan, J., Green, M. L. H. & Nicholas, R. J. 2006 Crystal-encapsulation-induced band-structure change in single-walled carbon nanotubes: photoluminescence and Raman spectra. *Phys. Rev. B* **74**, 245418. (doi:10.1103/PhysRevB.74.245418)

McCann, E. & Fal'ko, V. I. 2006 Landau-level degeneracy and quantum Hall effect in a graphite bilayer. *Phys. Rev. Lett.* **96**, 086805. (doi:10.1103/PhysRevLett.96.086805)

McClure, J. W. 1956 Diamagnetism of graphite. *Phys. Rev.* **106**, 666–671. (doi:10.1103/PhysRev.104.666)

Novoselov, K. S., Geim, A. K., Morozov, S. V., Jiang, D., Zhang, Y., Dubonos, S. V., Grigorieva, I. V. & Firsov, A. A. 2004 Electric field effect in atomically thin carbon films. *Science* **306**, 666–669. (doi:10.1126/science.1102896)

Novoselov, K. S., Geim, A. K., Morozov, S. V., Jiang, D., Katsnelson, M. I., Grigorieva, I. V., Dubonos, S. V. & Firsov, A. A. 2005 Two-dimensional gas of massless Dirac fermions in graphene. *Nature* **438**, 197–200. (doi:10.1038/nature04233)

Novoselov, K. S., McCann, E., Morozov, S. V., Fal'ko, V. I., Katsnelson, M. I., Zeitler, U., Jiang, D., Schedin, F. & Geim, A. K. 2006 Unconventional quantum Hall effect and Berry's phase of 2_{π} in bilayer graphene. *Nat. Phys* **2**, 177–180. (doi:10.1038/nphys245)

Park, C.-H., Giustino, F., Cohen, M. L. & Louie, S. G. 2007 Velocity renormalization and carrier lifetime in graphene from the electron–phonon interaction. *Phys. Rev. Lett.* **99**, 086804. (doi:10.1103/PhysRevLett.99.086804)

Reich, S., Thomsen, C., Maultzsch, J. & Ordejón, P. 2002 Tight-binding description of graphene. *Phys. Rev. B* **66**, 035412. (doi:10.1103/PhysRevB.66.035412)

Sadowski, M. L., Martinez, G. & Potemski, M. 2006 Landau level spectoscopy of ultrathin graphite layers. *Phys. Rev. Lett.* **97**, 266405. (doi:10.1103/PhysRevLett.97.266405)

Saito, R., Fujita, M., Dresselhaus, G. & Dresselhaus, M. S. 1992 Electronic structure of chiral graphene tubules. *Appl. Phys. Lett.* **60**, 2204–2206. (doi:10.1063/1.107080)

Saito, R., Dresselhaus, G. & Dresselhaus, M. S. 1998 *Physical properties of carbon nanotubes*. London, UK: Imperial College Press.

Wallace, P. R. 1947 The band theory of graphite. *Phys. Rev.* **71**, 622–634. (doi:10.1103/PhysRev.71.622)

Zhang, Y., Tan, Y. W., Stormer, H. L. & Kim, P. 2005 Experimental observation of the quantum Hall effect and Berry's phase in graphene. *Nature* **438**, 201–204. (doi:10.1038/nature04235)

Zhang, Y., Jiang, Z., Small, J. P., Purewal, M. S., Tan, Y.-W., Fazlollahi, M., Chudow, J. D., Stormer, H. L. & Kim, P. 2006 Landau-level splitting in graphene in high magnetic fields. *Phys. Rev. Lett* **96**, 136806. (doi:10.1103/PhysRevLett.96.136806)

Zhou, S. Y. *et al.* 2006 First direct observation of Dirac fermions in graphite. *Nat. Phys.* **2**, 595–599. (doi:10.1038/nphys393)